PHYSICAL REVIEW B VOLUME 37, NUMBER 8 15 MARCH 1988-I

Magnetooptics and excitation spectroscopy: Two efficient methods for distinguishing excitons bound to different acceptor centers in CdS

J. Gutowski and A. Hoffmann
Institut für Festkörperphysik, Technische Universität Berlin, Hardenbergstrasse 36, D-1000 Berlin 12, West Germany

(Received 8 June 1987; revised manuscript received 10 August 1987)

A set of sharp emission lines, $I_1^f-I_1^n$, is found in CdS crystals between the prominent I_1 and I_2 luminescence transitions which are due to the recombination of excitons bound to neutral acceptors and donors, respectively. By means of magnetooptical investigations and excitation spectroscopy, it is demonstrated that the lines $I_1^f-I_1^n$ are neither correlated with that acceptor-exciton complex which is the origin of I_1 nor with structurally identical complexes that only involve chemically different acceptor elements. They are explainable as radiative recombinations of excitons bound to a class of complicated centers. Up to now these centers have hardly been discussed in the creation of acceptor-exciton complexes in CdS. Zeeman splittings of $I_1^f-I_1^n$ and the analysis of their diamagnetic shifts allow for the discussion of the structure of these centers. Excitation spectra bring out information on their electronic excited states.

I. INTRODUCTION

Optical transitions of bound excitons in II-VI compounds have been shown to play an important role not only under low-density excitation conditions, but also in the high-density range. In CdS prominent examples are the I_1 lines due to the radiative recombination of excitons bound to Li- (line I_1^b) and Na-related (line I_1^a) acceptor centers.[1] Forbidden transitions I_1^i into excited electronic states of these complexes give rise to pronounced nonlinearities in the I_1 excitation spectra[2] as well as to resonant phononic[3] and electronic Raman scattering.[4–6] However, the variety of bound-exciton transitions in CdS complicates the analysis of experimental data. For example, the resonances I_1^i occurring in the I_1 excitation spectra taken under high-density excitation are found in the same energy regime where intentionally doped crystals show F-related[7] and P-related[1,8,9] bound-exciton luminescence structures. Thus several authors[10] argued that the I_1^i resonances could be attributed more to the creation of acceptor-exciton complexes involving chemically different impurity centers than to really excited electronic states of one single type of such a complex.

Now, we found that most of those CdS crystals which are not intentionally doped but exhibit strong I_1 luminescence lines show, on their high-energy side, well resolvable sets of luminescence structures already under low-density as well as under high-density excitation, although they are often relatively weak.

We have demonstrated in a series of papers[2,6,11] that excitation spectroscopy and magnetooptics of both luminescent transitions and excitation resonances are unrenouncable means to analyze the various creation and recombination channels of acceptor-exciton complexes. We investigated systematically the new sets of luminescence lines using these techniques. The results indicate that these lines may be of extraordinary importance since they are due to a special class of bound excitons in CdS involving complex acceptor centers instead of simply structured impurities. We will demonstrate that this manifold of lines offers excellent data to analyze complicated bound-exciton systems. Zeeman splitting and a giant diamagnetic shift behavior are discussed in terms of n-particle complexes with $n > 4$. This number of particles exceeds that in simple bound-exciton complexes, which alone have been proved to exist in CdS up to now. Furthermore, the new luminescence lines are definitely not correlated with the I_1^i resonances. Thus, we will show that the interpretation of the I_1^i excitation resonances in terms of excited (A^0,X) states remains valid.

II. EXPERIMENT

The samples were high-quality platelets with thicknesses between 50 and 500 μm, grown by the group of Dr. R. Broser (Fritz-Haber-Institut of the Max-Planck-Gesellschaft, Berlin). They have not been intentionally doped. Spectra have been taken under low-density conditions using the 476.5-nm emission of a 4-W Ar^+-ion laser (Spectra Physics). Temperature and magnetic-field dependence have been measured with this laser serving as light source. High-density spectra have been recorded under excitation with a pulsed dye laser pumped by an excimer laser (Lambda Physik). This system has been used for intensity-dependent measurements and excitation spectroscopy. The spectral half-width of the dye laser beam amounts to less than 0.005 nm with 15-ns pulse duration and maximum pulse intensities of some MW/cm^2.

The samples were immersed in liquid He at 1.5 K, except for the temperature-dependent measurements that have been performed in a continuous He flow of variable temperature. The experiments in a magnetic field have been carried out using a 15-T superconducting magnet built in the split-coil technique (Intermagnetics and Janis, Inc.).

The geometrical arrangement has been varied between backward and right-angle configuration. Light from the crystals has been decomposed in a 0.75-m double monochromator with 0.008-nm resolution (Spex Industries). The spectra have been supervised by an optical spectrum analyzer system (manufactured by B&M) to avoid scattering lines to be misinterpreted as excitation resonances. They have been recorded with a photomultiplier to yield highest resolution.

III. EXPERIMENTAL RESULTS

Figure 1 shows a typical spectrum obtained under low-density excitation (10 W/cm^2) with the 476.5-nm Ar-laser emission. I_1 together with its acoustic-phonon sideband I_1-TA is the dominant luminescence often exhibiting a doublet structure (not resolved in Fig. 1, compare with Fig. 2). This doublet called I_1^a and I_1^b is known to be due to two chemically different acceptor centers most probably correlated to Li and Na.[1] These two elements give rise to a very small difference in the bound-exciton binding energies of around 0.25 meV.

At around 487 nm, a set of lines I_2 is observable. I_2 is the radiative recombination of an exciton bound to a neutral donor. Strong chemical shift effects are well known to produce a variety of nearby lying lines of that nature.[10–12] The region of interest for the present paper lies between I_2 and I_1. As visible in Fig. 1, a manifold of very sharp lines called I_1^f–I_1^n is found between 487.5 and 488.5 nm. The polarization of all lines is strictly E⊥c, as that of the I_1 doublet. The intensity of these lines is a factor of 10 smaller than that of I_1. However, in other samples this ratio often is even less. The wavelengths and energy positions of all lines are listed in Table I, in comparison with known values of the I_1^i excitation resonances[2] of the lines $I_1^{a,b}$ and of the luminescence lines observed in intentionally P-doped samples.[7–9] As is seen from the table, $I_1^{g'}$ and I_1^l coincide with the two lines identified to be P related in doped samples. However, in our case, $I_1^{g'}$ is not the dominant line, and I_1^l is weak. Obviously, the occurrence of these further lines is not simply explainable with P impurities. This will be discussed in detail later. In regard to the I_1^i resonances, any coincidence with the luminescence lines seems to be accidental. Although I_1^f, I_1^g, and I_1^l are found at the same energies as I_1^2, I_1^3, and I_1^4, respectively, just the strongest lines I_1^g and I_1^h do not correspond to any of the I_1^i excitation maxima. Any systematic correlation should be excluded between the luminescences and resonance lines.

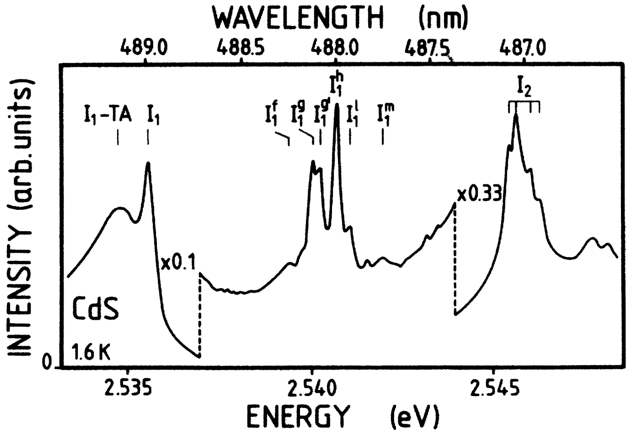

FIG. 1. Luminescence spectrum of CdS in the energy range of bound-exciton transitions, taken under excitation with light of the 476.5-nm emission of an Ar-ion laser, with intensity 10 W/cm^2.

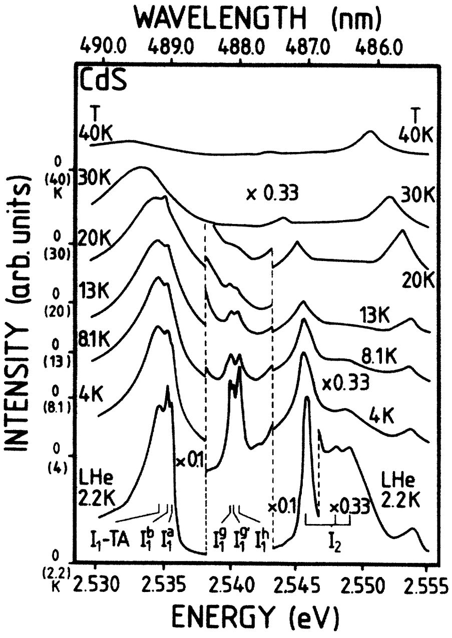

FIG. 2. Luminescence spectra in the exciton energy range under Ar-laser excitation for different crystal temperatures. LHe in the lowest curve (2.2 K) means "measured in liquid helium."

Figure 2 presents the temperature dependence of all lines visible between the free A exciton and the I_1-TA sideband of I_1. It is evident that all I_1^f–I_1^n lines disappear between 30 and 40 K as do the bound-exciton lines I_1 and I_2. This behavior is generally known for excitons bound to neutral impurities in CdS. It has been interpreted on the basis of ionization processes of neutral centers under recombination of the electrons via intermediate states becoming important above 30 K.[13] As opposed to these transitions, the A exciton luminescence being weak compared with the bound-exciton lines at 2.2 K remains visible up to more than 40 K as is expected for free-exciton-related transitions.

The intensity dependence of the luminescence spectra is demonstrated in Fig. 3. In the lowest curve, the spectrum presented in Fig. 1 is again reproduced. The Ar-ion laser irradiation amounts to 10 W/cm^2. The upper spectra have been recorded under pulse laser excitation. The middle spectrum obtained for 3.9 kW/cm^2 is very similar to the cw spectrum. The I_1-TA band is more pronounced, and the I_2 line quartet is distorted by a broader luminescence band beginning to emerge on its low-energy side.

TABLE I. Wavelengths λ and energies E of I_1^f–I_1^n luminescence lines. Binding energies E_B are calculated with respect to the energy of the free A_F exciton (2.5519 eV). The data are compared with the values of the I_1^i excitation resonances measured in the excitation spectra of the I_1 transition (Ref. 2), and luminescence lines of intentionally P-doped samples. No systematic correlation between the new luminescence lines and the excitation resonances could be found.

Line	λ (nm)	E (eV)	E_B (meV)	I_1 excitation resonance[a] E (eV)	Lines in P-doped samples[b] E (eV)
				2.5381I_1^1	
I_1^f	488.253	2.539 36	12.54	2.5393I_1^2	
I_1^g	488.127	2.540 02	11.88		
$I_1^{g'}$	488.086	2.540 23	11.67	2.5402I_1^3	2.540 26
I_1^h	487.995	2.540 71	11.19		
I_1^l	487.930	2.541 04	10.86	2.5412I_1^4	2.541 01
I_1^m	487.795	2.541 75	10.15		
I_1^n	487.650	2.542 50	9.40	2.5422I_1^5	
				2.5439I_1^6	
I_1^a	488.976	2.535 61	16.29		
I_1^b	489.011	2.535 43	16.47		

[a] Reference 2.
[b] Reference 1.

At 150 kW/cm^2, drastic changes are detectable. Between I_2 and the I_1^f–I_1^n lines, the prominent M band appears due to biexciton recombination processes.[14] It increases strongly superlinearly with growing excitation density, in contrast to the lines I_1^f–I_1^n which are partly disappearing in the rising low-energy tail of M. I_1 and I_1-TA luminescences show a beginning stimulated emission. On their low-energy side, the P bands occur which have been controversially discussed in terms of biexciton recombination or exciton-exciton scattering processes.[14]

In conclusion, the lines I_1^f–I_1^n do not present an intensity behavior which would be specific for high-density phenomena, again in contrast to the I_1^i excitation resonances of the $I_1^{a,b}$ transitions.[2]

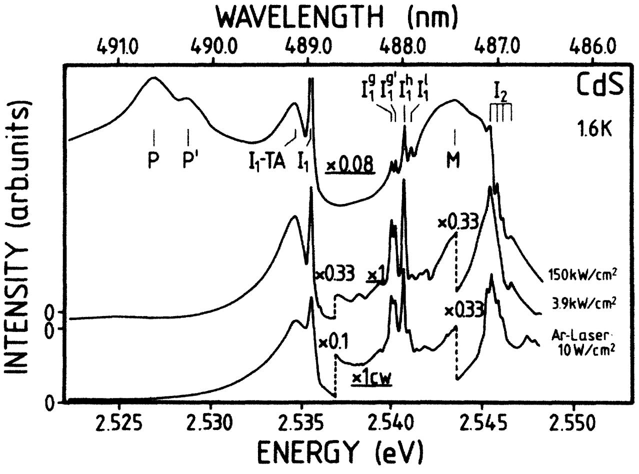

FIG. 3. Luminescence spectra for three different excitation densities. The lower spectrum has been taken under cw excitation with the 476.5-nm line of the Ar laser. The upper spectra were recorded under pulse dye laser excitation. The laser wavelength was 485.5 nm. Intensities are not quantitatively comparable between the cw and the pulse spectra. Factors being underlined are referred to the whole spectrum, respectively.

The behavior of the main lines I_1^g–I_1^l in a magnetic field is illustrated in Fig. 4, in comparison with that of the $I_1^{a,b}$ doublet. Obviously, pronounced differences are recognizable between these two types of lines. For **B**⊥**c**, $I_1^{a,b}$ show the typical doublet splitting with the unpaired electron g value of 1.72, which is most clearly in agreement with the literature.[13,15] For **B**||**c**, we obtain $g = 1.80$ which is larger than the values reported earlier. However, the thermalization behavior in each magnetic-field configuration doubtlessly underscores the assignment of both lines to acceptor-bound excitons.

I_1^g–I_1^l possess very different Zeeman patterns especially for **B**⊥**c**. The strongest line, I_1^h, exhibits a fourfold splitting. The occurrence of a fifth low-energy component as traced in the figure is doubtful, since this component is extremely weak and may be of other origin than

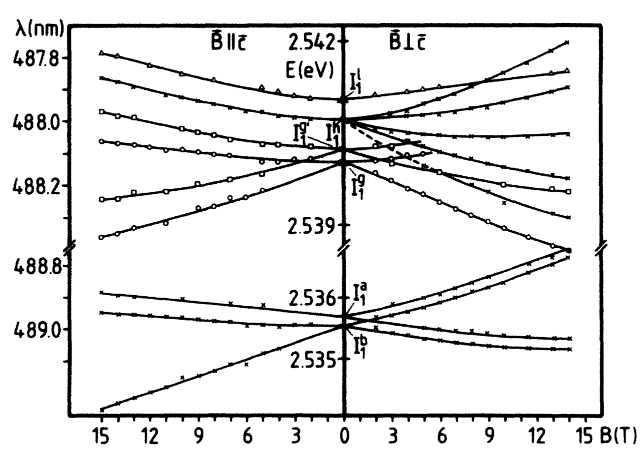

FIG. 4. Zeeman splitting of the lines $I_1^{a,b}$ and I_1^g–I_1^l in a magnetic field in Voigt configuration **k**⊥**c**.

TABLE II. g values and thermalization of $I_1^f - I_1^n$ lines in a magnetic field. The data are compared with those obtained from investigations of the I_1^i excitation resonances (Refs. 2 and 16). It is evident that the luminescence lines behave completely different to the excitation resonances. For each multiplet the thermalization is given below the g values. The meaning of symbols is $l+$, low-energy component; $h+$, high-energy component is the stronger line; no therm, no thermalization observable.

	B$\|\|$c	**B**$\perp$c	**B**$\|\|$c	**B**$\perp$v
			I_1^2 doublet	doublet
			0.74	1.77
			no therm	$l+$
I_1^g	1.79	2.28		
	$h+$	$l+$		
$I_1^{g'}$	1.65	1.66	I_1^3 doublet	triplet
	$h+$	$l+$	0.87	2×1.68
			$h+$	$l+$
		fourfold		
I_1^h	(0.78)	2.73		
	$h+$	$l+,l+$		
			I_1^4 doublet	triplet
I_1^l	unsplit	unsplit	0.80	2×1.72
			no therm	no therm
I_1	1.80	1.72		
	$h+$	$l+$		

the strong quartet at higher energies. I_1^g and $I_1^{g'}$ are only twofold split while I_1^l seems to remain unsplit. The low-energy components are the stronger ones for all split lines in **B**$\perp$c which means that the initial state always has the larger g value.

For **B**$\|\|$c, I_1^g and $I_1^{g'}$ again are twofold split while I_1^h and I_1^l seem only to shift to higher energies. A second component for each of the latter lines can be assumed to lie at lower energies provided it is thought to be very weak and superimposed by the strong lines originating from the other transitions at low temperatures. This assumption may be reasonable, since in the **B**$\|\|$c configuration each split line I_1^g and $I_1^{g'}$ has a considerably more intensive high-energy component. Thus for all lines the respective final states are expected to possess the larger g values.

All g values and thermalization properties are listed in Table II, compared with those of the coinciding I_1^i resonances (data from Ref. 16). If, e.g., $I_1^{g'}$ and I_1^l are compared with the excitation resonances I_1^3 and I_1^4, respectively, it becomes evident that their behavior is completely different. This emphasizes the fact that the energetic coincidence between some resonances and luminescence lines is accidental.

The diamagnetic shifts of the Zeeman multiplets give further important information on the complexes involved. Table III shows the values measured compared with theoretical estimations which will be explained and discussed in Sec. IV. The experimental values are calculated from the quadratic deviations of the center of gravity of each multiplet from its linear shift sometimes observable for low fields. It is remarkable that the shifts obtained for $I_1^g - I_1^n$ are, in general, larger than those known from $I_1^{a,b}$ and I_2.

Excitation spectra of the luminescence lines yield information about the creation channels of the complexes involved. However, excitation spectra with polarization **E**$\perp$c of the exciting laser are hardly recordable due to the excellent excitability of the M luminescence in the energy range of interest. This band strongly superimposes the $I_1^f - I_1^n$ lines even for those excitation densities for which

TABLE III. Diamagnetic shifts of bound-exciton luminescence lines, experimental and theoretical values. The basis of the theoretical estimations is explained in Sec. IV.

	B$\|\|$c		**B**$\perp$c	
	Theory δ_{th} (μeV/T^2)	Expt. δ_{ex} (μeV/T^2)	Theory δ_{th} (μeV/T^2)	Expt. δ_{ex} (μev/T^2)
Single acceptor	0.000 46		0.021	
Single donor	0.56		0.56	
Free exciton X	0.72		1.42	
I_1 (A^0,X)	0.43	0.31	1.22	1.28
I_2 (D^0,X)	0.78	0.76	1.71	1.12
I^g	0.76	1.29	1.75	1.48
$I^{g'}$	0.76	1.20	1.75	1.48
I^h		2.7		3.11

excitation resonances of $I_1^f - I_1^n$ analogous to the I_1^i maxima of I_1 would have been expected. Thus at higher densities data may not be reliable to form the basis for adequate interpretations. For very low intensities, however, no interesting structures are visible in the excitation spectra of $I_1^f - I_1^n$ except for free exciton resonances. Therefore, excitation spectra have been preferably taken for E||c polarization of the incident light. Figure 5 shows spectra of I_1^a, I_1^h, and I_1^g. All lines are excitable via the free A_L longitudinal (2.554 06 eV) and the A_F triplet exciton (2.551 83 eV). A_L is seen as a complicated resonance feature exhibiting a dip exactly coinciding in energy in all three excitation spectra but for I_1^g and I_1^h posed on an excitation maximum feature. This occurrence of a dip may be due to strong reflection and surface absorption just at the A_L energy maximum which prevents the efficient creation of excitons in the bulk, whereas efficient excitation is possible in the A_L tails. A_F, however, is seen as an extremely sharp maximum preferably in the I_1^g and I_1^h spectra. Since this exciton is dipole forbidden for $k = 0$ it is only visible due to the slight deviation of the photon's k from zero, resulting in a weak absorption in the bulk crystal. Obviously, this is followed by an efficient excitation of bound excitons.

On the low-energy side of the free exciton transitions, I_1^a, I_1^g, and I_1^h exhibit completely different resonances. I_1^a shows the well-known set of resonances between 2.548 24 and 2.550 94 eV (the resonance energies are listed in Table IV) in the regime of the electronic ground states of the (A^0,X_B) complex. This complex involves one hole from the second B valence band in CdS, indicated by the subscript B. Its electronic ground state has been analyzed in detail in Refs. 6 and 11.

In the excitation spectrum of I_1^h a quartet structure is seen between 2.549 52 and 2.551 18 eV (see Table IV), being similar to that discussed above for I_1^a. Again, at the low energy side two sharp lines are observable, followed by two broader resonances at higher energies. However, compared with the resonances of I_1, the whole set of maxima is shifted to higher energies, and the distances between the different maxima are considerably smaller than those obtained for the four resonances of I_1^a.

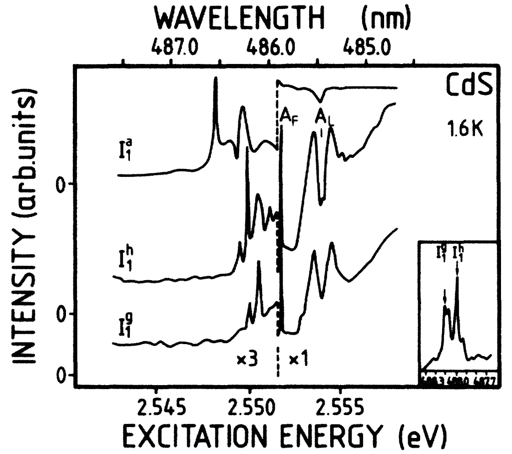

FIG. 5. Excitation spectra of I_1^a, I_1^g, and I_1^h (luminescence spectrum shown in the inset of the figure) under pulse laser light. For the description of the various excitation resonances, see text.

The excitation spectrum of I_1^g again shows such a characteristic set of resonances below the free excitons. However, although I_1^g is lower in energy than I_1^h, its respective excitation resonances are further shifted to higher energies. Only two sharp lines are definitely detectable which are obviously analogous to the two sharp maxima seen in the spectra of I_1^h or I_1^a. The two broader resonances, which would be assumed to exist on the high-energy side of the sharp maxima, are probably superimposed by the very intense and sharp A_F reso-

TABLE IV. Excitation resonances of I_1^a, I_1^g, and I_1^h under polarization E_i||c of the incident light. All resonances except the free-exciton transitions A_F and A_L are obviously due to the creation of the three different acceptor-exciton complexes with one hole from the second B valence band. This kind of complex possesses a fourfold-split electronic ground state. It is evident that a set of resonances belongs to each of the three complexes represented by their recombinations I_1^a, I_1^g, and I_1^h, and that the resonances of the different complexes distinctly differ in energy. The relative distances ΔE are calculated with respect to the B polariton (2.5677 eV).

I_1^a		I_1^g		I_1^h	
E (eV)	ΔE (meV)	E (eV)	ΔE (meV)	E (eV)	ΔE (meV)
2.548 24	19.46				
2.549 02	18.68				
				2.549 52	18.18
2.549 72	17.98				
		2.550 01	17.69	2.549 92	17.78
		2.550 53	17.17	2.550 53	17.17
2.550 94	16.76				
		2.551 09	16.61		
				2.551 18	16.52
(2.5519)		2.551 83		2.551 83	
A_F		A_F		A_F	
2.554 06		2.554 06		2.554 06	
A_L		A_L		A_L	

nance.

In conclusion, from the features of all three spectra it becomes evident that on the low-energy side of A_F analogous sets of up to four resonances occur indicating a comparable physical nature. However, their differing resonance energies, as well as their different energy separations, doubtlessly show that the excitation channels of the three luminescence lines I_1^a, I_1^g, and I_1^h are not identical.

Table IV presents the absolute energy values for all three sets of resonances. The relative distances of the resonances to the B exciton energy are represented on the right-hand side of the table. To use the B exciton as a reference point is justified when one assumes that the resonances of the $I_1^{g,h}$ lines are also correlated with states involving one B valence-band hole.

IV. DISCUSSION

In this discussion we will establish that the luminescence lines located between I_1 and I_2 are not explainable by those kinds of bound-exciton systems which are, apart from the chemical nature of the acceptor, structurally identical with that causing the I_1 radiation. They are shown to belong to a class of bound exciton system with relatively complicated impurity centers.

A. Relation between the new bound-exciton luminescence lines and known excitation resonances

From the comparison of the energies and the magnetic-field dependence of the $I_1^f - I_1^n$ luminescences with the I_1^i excitation resonances, it has been concluded that no correlation exists between these two groups of transitions. They show only poor and accidental coincidences but mostly pronounced deviations. Moreover, it is not reasonable to apply the given interpretation of the I_1^i resonances[2] in terms of excited (A^0,X) states to the luminescence lines also. In general, radiative recombination out of excited states never occurs in luminescence spectra.[2,10,12] Competing nonradiative relaxation into the (A^0,X) ground state is much more probable and takes place within picoseconds or less.

The opposite idea is to explain the coincidental I_1^i resonances and $I_1^f - I_1^n$ luminescence lines both by the creation of chemically different bound exciton complexes. However, this is likewise unreasonable because of the severe deviations of the line's behavior. Moreover, all excitation resonances then should correspond to luminescent transitions being highly probable in this case.

In conclusion, it is evident that the luminescences $I_1^f - I_1^n$ are not correlated with the known I_1^i excitation resonances of the $I_1^{a,b}$ luminescence lines. Thus any reinterpretation of the latter lines with respect to new bound-exciton complexes is not appropriate. Therefore, we focus on the identification of the origin of the $I_1^f - I_1^n$ lines on the basis of the numerous experimental data.

B. General remarks to the experimental behavior and the origin of the $I_1^f - I_1^n$

All new lines are evidently connected with acceptor-bound-exciton complexes. From Table I, binding energies with respect to the free A exciton [A_F, 2.5519 eV (Ref. 17)] are calculated. Energies between 9.4 and 12.6 meV are relatively but not unusually small for acceptor-bound excitons in CdS as is seen from the data obtained using intentionally F-doped or P-doped samples.[1,8,9] The strongest arguments for an assignment of the $I_1^f - I_1^n$ lines to acceptor-bound-exciton systems are found first from the temperature dependence which is absolutely identical to that of known acceptor-exciton complexes in CdS. Second, the excitation spectra in $\mathbf{E} \| c$ are of strikingly similar structure as those of $I_1^{a,b}$ whereas excitation spectra of I_2 transitions (donor-bound excitons) are known to look completely different.[10,12] In detail, deviations exist in the excitation spectra of the various lines and offer interesting information as will be discussed later. Third, the thermalization behavior of $I_1^{g,h}$ under the influence of a magnetic field is identical with that of $I_1^{a,b}$ although splittings and shifts are very different. Initial and final states involved obviously exhibit some analogy. In contrast, I_2-like transitions show reversed thermalization properties[10,12] due to a reversed term structure of the initial and final states compared to (A^0,X) complexes. Furthermore, donor-exciton complexes are not expected to be as strongly bound as is derived for $I_1^f - I_1^n$. The bound-exciton binding energy is coupled to the impurity depth by the Haynes rule. The donor depth typically does not exceed 30 meV in CdS. From I_1^g, for example, a binding energy of 12.54 meV is derived which would be more than 40% of the donor depth. This is definitely untypical for any II–VI compound.

In conclusion, the origin of the $I_1^f - I_1^n$ lines in terms of the radiative recombination of excitons bound to neutral-acceptor–like centers is the most reasonable interpretation up to now.

C. Analysis of bound-exciton electronic states based on magnetic-field dependent data

1. Zeeman splitting

To go into detail, we now discuss the quantitative data obtained under the influence of a magnetic field. For $\mathbf{B} \perp c$, the most clear-cut situation is found with respect to I_1^h. The split quartet consists of two low-energy lines being equal in strength, and of two high-energy components again equal in strength, but with a decreasing intensity ratio relative to the low-energy doublet for increasing magnetic field. The only explanation is that the initial state, as well as the final state of the I_1^h transition, split into doublets, respectively. With regard to Fig. 6, four thermalized transitions have to be expected, in coincidence with the experiment. The g value of the initial-state doublet can be calculated from the experimental data given in Table II to be $g_u = 1.75$, whereas $g_l = 0.98$ is obtained for the final state (u represents the upper, l represents the lower state). The first value is identical with the free electron's g value in CdS measured already for the $I_1^{a,b}$ transitions.[2,15] This parallel is remarkable since neutral single acceptors always are centers with even numbers of charged particles involved (including the charge of the fixed ion center). If the hole of the bound

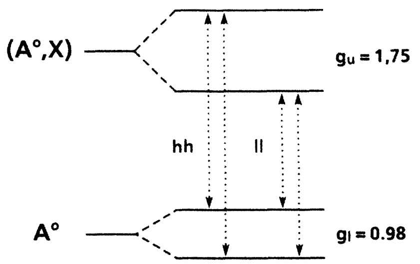

FIG. 6. Term scheme of the transition I_1^h with splitting in a magnetic field. The g values g_u for the upper level and g_l for the lower level are deduced from the experimentally measured splitting and thermalization of I_1^h. *ll* marks the lower-energy pair of split lines which are the stronger ones, the high-energy pair *hh* is weaker due to the depopulation of the upper split level of the (A^0,X) ground state.

exciton is paired with one hole within the acceptor center only, the exciton's electron remains necessarily unpaired. The splitting of the ground-state level of the (A^0,X) complex, therefore, only results from the splitting of this unpaired electron possessing Γ_7 symmetry and $s_z=\pm\frac{1}{2}$ spin orientation and behaving isotropic in CdS. So far, the situation is identical to that of the known Na and Li related (A^0,X) complexes (lines $I_1^{a,b}$) in CdS. However, their final states A^0 possess Γ_9 symmetry due to the single hole's $s_z=\pm\frac{3}{2}$ and remain unsplit. In contrast to this expectation, we measure a final state's split and allowed transitions into both ground-state levels from both $s_z=\pm\frac{1}{2}$ upper levels. Thus it is suggested that the acceptor's hole may not be the only mobile charge involved in the neutral center. This, and the consequences for the symmetry being reduced as well as for the transition's selection rules, will be discussed in Secs. IV C 2 and IV C 3 in connection with the diamagnetic shift data.

Similar ideas will hold with regard to I_1^g and $I_1^{g'}$ in **B**⊥**c**. Although they only show doublet splitting, the measured g values differ from the simple free-electron value. If the initial state is assumed again to be an (A^0,X)-like ground state with one unpaired electron, the final states will be calculated to split with $g_{l_\perp}=0.09$ and 0.53 for $I_1^{g'}$ and I_1^g, respectively.

For **B**||**c**, deviations from the behavior of $I_1^{a,b}$ are again recognizable. I_1^g and $I_1^{g'}$ show slightly smaller g values than $I_1^{a,b}$, connected with larger diamagnetic shift values. I_1^h is assumed to have a very weak low-energy component besides a strong high-energy component. Proposing once more that the unpolarized electron is responsible for doublet splits of the initial states in all cases, one calculates a g_l of 3.54 for the final state of the I_1^g transition, $g_l=3.40$ for $I_1^{g'}$, and $g_l=2.53$ for I_1^h. In contrast to that, the acceptor involved in the known (A^0,X) complexes splits with $g_l=2.7$ (Ref. 15) so that none of the new lines closely fits this result. As for **B**⊥**c**, the final state must be of another nature than that in the case of the $I_1^{a,b}$ lines. Nevertheless, thermalization again is in the closest agreement with that of $I_1^{a,b}$ underlining a certain relation to these kinds of transitions.

2. Diamagnetic shift and the number of particles in acceptor-exciton complexes

A further key to the understanding of the nature of the complexes may be the diamagnetic shift behavior. Stébé *et al.*[18] have developed a theory to calculate diamagnetic shifts of bound-exciton transitions depending upon the number of particles involved in one complex and of their effective masses. Although they made use of a simple nondegenerate isotropic two-band model, they could show that their results are in principle applicable to the more difficult situation of II-VI compounds like CdS. They started from a diamagnetic operator

$$H_D=\tfrac{1}{8}\gamma_A^2\left[\sum_{h=1}^{n_h}\rho_{h1}^2+\sigma^{-1}\sum_{e=1}^{n_e}\rho_e^2\right], \tag{1}$$

with $\sigma=m_e^*/m_h^*$, and $\rho_i^2=x_i^2+y_i^2$ for the (A^0,X) complex with n_h holes and n_e electrons involved. γ_A is defined as

$$\gamma_A=\hbar\omega_c/2\,|E_A|\;, \tag{2}$$

with $\omega_c=eB/m_n^*c$ the effective hole cyclotron frequency and E_A the acceptor ionization energy. With

$$\gamma_X=\gamma_A(1+\sigma^{-1})^2 \tag{3}$$

for the free exciton X, the diamagnetic energy shift is derived to be

$$\Delta E_A=\gamma_A^2\,|E_A|\,/2 \tag{4}$$

for the acceptor and to be

$$\Delta E_X=\gamma_X^2\,|E_X|\,/2 \tag{5}$$

for the free exciton with E_X being its binding energy. The shift $\Delta E(A^0,X)$ then is calculated numerically with respect to ΔE_A or ΔE_X and different σ. From those data we receive

$$\Delta E(A^0,X)=0.87\Delta E_X \tag{6}$$

for CdS. Taking into account the anisotropy of CdS and assuming the low-field limit of around 10 T (specified in Ref. 18) not to be considerably exceeded in our measurements (15 T maximum), we receive the data for I_1 and I_2, which are given in Table III, in comparison with the experimental values. An excellent agreement of experiment and theory is remarkable for I_1 and I_2 although the theoretical approach is rough. Second, the experimental shifts of $I_1^{g,g',h}$ are considerably larger than those of I_1 and partly of I_2 which indicates that, following Eq. (1), more than three mobile particles have to be involved in the acceptor-exciton complex.

3. Application to the $I_1^f - I_1^n$ luminescent transitions: suggestions to the nature and structure of the bound excitons involved

Henry *et al.*[1] proposed that their I_1-like lines situated around 488 nm are caused by excitons bound to a complex acceptor center of low symmetry involving P. In contrast to that, it was argued that single P atoms gave rise to deep acceptor centers in CdS. Only two lines are identified in Ref. 1 which coincide with I_1^l and $I_1^{g'}$, but they possess completely other intensity ratios. Nevertheless, centers of low symmetry are obviously responsible for all complexes related to $I_1^f - I_1^n$ since in all cases the final states show a splitting for **B**⊥**c**, too.

With respect to the magnetic-field dependent data, we discuss in the following the centers which are composed of two impurities which together act on the exciton as an acceptor. Acceptor complexes consisting of a Cd vacancy V_{Cd}^{2-} and an interstitial donor D_{is}^{+} in principle have been proposed by Refs. 1 and 7 to bind excitons in CdS. However, since a Cd vacancy is a deep double acceptor, its holes should not considerably influence the diamagnetic shift of the system consisting of the exciton-impurity complex. Thus instead of the deep vacancy, a more shallow acceptor impurity may be involved in such a complex which is then called $A_{\mathrm{Cd}}D_{\mathrm{is}}$ and is thought to be responsible for the $I_1^f - I_1^n$ lines. Three mobile charges must be involved in such a system if the diamagnetic shift is to be enlarged and has to be calculated in the effective-mass approximation used by Stébé *et al.*[18] Two holes stem from the impurity which represents the double acceptor, one electron neutralizes the positive and fixed charge D^+. This model fits with the observed experimental behavior of the lines in a magnetic field; in particular, since a hole of such an acceptor cannot be described in C_{6v}^{+} as possessing Γ_9 symmetry. The symmetry of such a pair $A_{\mathrm{Cd}}D_{\mathrm{is}}$ is reduced to C_s or, in the case of orientation of its axis along c, to C_6. In C_s the neutral-acceptor complex is represented by $\Gamma_3+\Gamma_4$, as is the acceptor-exciton complex in its ground state. Both are split in a magnetic field **B**⊥**c**, and four transitions are expected to occur in agreement with the experimental Zeeman pattern of I_1^h. For I_1^g and $I_1^{g'}$, the final state has been shown to split, too. Thus a structure of the acceptor center similar to that involved in I_1^h has to be assumed. The fact that only two transitions are observable for each line in the B field can be a question of orientation of the $A_{\mathrm{Cd}}D_{\mathrm{is}}$ pair. For example, in C_6 only two of the four possible transitions are optically allowed for momentum selection rules although the acceptor ground state likewise splits in **B**⊥**c**. A C_6 symmetry is also favored with regard to the polarization properties of the transitions. While a symmetry reduction to C_6 does not alter the transition selection rules, all transitions between the (A^0,X) ground state and the A^0 centers remain strictly polarized **E**⊥**c**, also transitions polarized **E**||**c** are allowed after a reduction to C_s. A contribution of light polarized parallel to c, however, has been observed neither for I_1^g, and $I_1^{g'}$ or I_1^h. Thus the symmetry of the complex involved in I_1^h is not finally clear.

The distance between I_1^g and $I_1^{g'}$ amounts to 0.04 nm. Since their Zeeman patterns are extremely similar, they should be due to two acceptor centers equal in structure and orientation. The only difference will be the chemical nature of the donor or acceptor element. This is analogous to the occurrence of the two nearby lines I_1^a and I_1^b where Li and Na on Cd are known to act as single acceptors.

The diamagnetic shift of the pure $A_{\mathrm{Cd}}D_{\mathrm{is}}$ complex as well as that of the system consisting of this complex and a bound exciton can be estimated from Eq. (1) if the full number of mobile electrons and holes is inserted. What can be observed experimentally is the difference of both shifts. The theoretical values of 0.76 μeV/T^2 for **B**||**c** and 1.75 μeV/T^2 for **B**⊥**c** are compared with the experimental data in Table III. A reasonable agreement is obtained if the estimation is kept in mind to be very rough. I_1^h, however, exhibits a larger shift in both configurations. This may be explained by the participation of more than three mobile particles in the neutral-acceptor complex.

It was shown in Ref. 1 that only very few elements of those coming into question to be present during the CdS growth are really able to be incorporated substitutionally as well as interstitially. Li and Na have radii suitable and small enough to fill up an interstitial site. These elements are known to form shallow acceptors in CdS if they substitute a Cd atom, as was described above. The diamagnetic shift, the splitting data, and the symmetry considerations are reasons to interpret the lines $I_1^f - I_1^n$ in terms of $A_{\mathrm{Cd}}\mathrm{Li}_{\mathrm{is}}$ and $A_{\mathrm{Cd}}\mathrm{Na}_{\mathrm{is}}$ acceptor-bound excitons with different orientations of the impurity pair axis to the crystal c axis. This is also underlined by the fact that I_1^g and $I_1^{g'}$ exhibit a chemical shift comparable to the $I_1^{a,b}$ doublet. The acceptor center involved in I_1^h may even be of multiparticle nature. For the remaining lines, no detailed assignment is possible due to their relative weakness which has prevented satisfactory data in a magnetic field. However, they may belong to the same kind of complex but with chemically different donors. No other explanation is reasonable because of their very similar binding energies and coinciding intensity and temperature behavior. This model also explains that all lines occur with very different intensity ratios in different crystals. It is immediately understandable that they are only observable in samples exhibiting strong $I_1^{a,b}$ luminescence if Na and Li are necessary to build up these complexes.

The fact that the exciton obviously is more weakly bound to these complexes than to single-atom acceptors shows that the mean field of such a center is reduced compared with the dipole field of the single-atom A^0 center. This is absolutely reasonable with regard to theory of electric fields caused by multiple-charge systems. However, exact calculations are expected to be extremely difficult, and are still restricted to four-particle problems resulting from an exciton–single-atom-acceptor complex up to now.[19]

D. Excitation channels and excited states of the new bound-exciton complexes

The given explanation for the $I_1^f - I_1^n$ lines is also confirmed by the analysis of the excitation spectra of I_1^g and I_1^h. An analogy in the resonance term's structure is observable in comparison with the excitation spectrum of I_1^a. In this spectrum the four resonances below the free exciton's energy have been attributed[11] to states of the same complex but involving one hole from the B valence band [this complex is called (A^0,X_B)]. If the complex is created in such a state, a fast $B \rightarrow A$ hole conversion results in the strong resonant enhancement of the respective recombination line.[11] An (A^0,X_B) electronic ground state in CdS is fourfold split by hole-hole and electron-hole exchange interactions. Four lines are theoretically expected to exist; two sharp and two broader lines. These lines should build two doublets. In the case of the acceptor-exciton complex related to the I_1^a transition, each should exhibit an inner line distance of less than 40 μeV being unresolvable. Thus the experimental observation of two clearly resolvable doublets[11] is due to transitions into two chemically different (A^0,X_B) complexes caused by chemical shifts also responsible for the occurrence of the $I_1^{a,b}$ doublet. Therefore, the doublets could be attributed to Li- and Na-related (A^0,X_B) complexes, respectively.

The fact that similar resonances are observable with regard to I_1^g and I_1^h shows that all bound-exciton complexes, independent of the chemical nature of the impurity, can also be built with one hole stemming from the second B valence band in CdS. However, the excitation resonances of I_1^g and I_1^h are found at higher energies than those of $I_1^{a,b}$. This unambiguously shows that the $I_1^f-I_1^n$ lines have to be assigned to (A^0,X) complexes being different from those causing $I_1^{a,b}$, and cannot be related with their excited states. Moreover, this means that excitons with a B hole are bound to these $A_{\mathrm{Cd}}D_{\mathrm{is}}$ centers with energies obviously smaller than those of excitons at single-atom acceptor centers, as was the case for excitons with A holes ($I_1^f-I_1^n$ lines themselves compared to $I_1^{a,b}$; compare ΔE from Table IV to E from Table I). However, whereas the differences of the binding energies between the (A^0,X_A) complexes correlated to $I_1^{a,b}$ on the one hand and to $I_1^f-I_1^n$ on the other hand are large (up to 4 meV), those of the (A^0,X_B) complexes related to the sets of excitation resonances are less pronounced (up to 1.5 meV). This indicates that the binding energies of (A^0,X_B) complexes may not be that sensitive to the chemical and structural nature of the impurity centers as are the binding energies of (A^0,X_A) complexes.

Furthermore, it is interesting to notice that some properties of the chemical shift of excitons bound to neutral acceptors which have been found in connection with the single-atom centers[11] are also observable at these complex centers. With regard to the energy position of the excitation maxima of I_1^g and I_1^h, one derives that the binding energies of B excitons in the $(A^0_{A\text{-}D},X_B)$ complexes behave opposite to those in the respective $(A^0_{A\text{-}D},X_A)$ complexes with the exciton's hole originating from the upper A valence band. Namely, the higher-energy transition I_1^h possesses excitation resonances lying lower in energy than the respective maxima of the lower-energy line I_1^g. The same behavior has been observed with respect to I_1^a and I_1^b involving the single-atom Li and Na acceptor centers.[11] This was explained by us[11] with the changing distance between the exciton and the impurity center if an A exciton is replaced by a B exciton. The resulting variations in the binding energy underlie opposite tendencies of the chemical shifts of (A^0,X_A) and (A^0,X_B) complexes, respectively. This observation may give additional information for theoretical treatments of this phenomenon based on the model of central-cell corrections.

V. SUMMARY AND CONCLUSIONS

In CdS crystals which exhibit relatively strong acceptor-bound exciton luminescence, we observed sets of luminescence lines between the donor-exciton recombination I_2 and the prominent acceptor-exciton lines I_1. The differing intensity ratios of these lines $I_1^f-I_1^n$ in various crystals indicated that they may belong to various discernable acceptor-exciton complexes. Mainly their excitation spectra and their behavior in a magnetic field showed that they are not explainable assuming chemically different but simple (e.g., single-atom) acceptor centers to be involved. The final states of all transitions showed definite Zeeman splittings that contrasts expectation when single-atom centers would be assumed. From binding energies, Zeeman g values, and for crystal symmetry reasons, we could assign the luminescence lines to the recombination of excitons from $(A^0_{A\text{-}D},X)$ centers where the neutral-acceptor center is composed of a double acceptor and a donor at interstitial site. The donor has been derived to be Li or Na. Some of the new lines have been identified to be due to the chemical shift caused by these two different elements in such a $A_{\mathrm{Cd}}\mathrm{D}_{\mathrm{is}}$ complex. Moreover, an opposite tendency of the chemical shift has been found when A or B excitons are bound to these two complexes. This is in agreement with similar observations at the prominent $I_1^{a,b}$ lines in CdS.[11]

We could show by comparison of excitation spectra and Zeeman splitting, that the lines $I_1^f-I_1^n$ are not correlated with the I_1^i resonances earlier observed in the excitation spectra of $I_1^{a,b}$. Thus the interpretation of the excitation resonances in terms of excited (A^0,X) states involving a single-atom acceptor is not affected by our experimental findings reported now.

The $I_1^f-I_1^n$ lines offer new possibilities to investigate the structure of bound-exciton complexes in CdS since they represent complicated but well-investigated systems. It would be desirable to perform a respective analysis also in other II–VI compounds to get complete information on the characteristics of these complexes more independent of the host compound.

ACKNOWLEDGMENTS

The authors wish to thank Dr. R. Broser for supplying the crystals and Professor Dr. I. Broser for helpful discussions and a critical reading of the manuscript. This work has been partly supported by the Deutsche Forschungsgemeinschaft.

[1] C. H. Henry, K. Nassau, and J. W. Shiever, Phys. Rev. B **4**, 2453 (1971).

[2] R. Baumert, I. Broser, J. Gutowski, and A. Hoffmann, Phys. Rev. B **27**, 6263 (1983).

[3] R. Baumert, I. Broser, J. Gutowski, and A. Hoffmann, Phys. Status Solidi B **116**, 261 (1983).

[4] D. Munz and M. H. Pilkuhn, Solid State Commun. **36**, 295 (1980).

[5] I. Broser and J. Gutowski, *International Conference on Luminescence, Madison, Wisconsin,* 1984 [J. Lumin. **31/32**, 397 (1984)].

[6] J. Gutowski and I. Broser, Phys. Rev. B **31**, 3621 (1985).

[7] D. G. Thomas, R. Dingle, and J. D. Cuthbert, *Proceedings of the 7th International Conference on II–VI Semiconducting Compounds, Providence* (Benjamin, New York, 1967), p. 863.

[8] K. Colbow and K. Yuen, Can. J. Phys. **50**, 1318 (1971).

[9] Y. Shiraki, T. Shimada, and K. Komatsubara, J. Phys. Chem. Solids **38**, 937 (1977).

[10] J. Puls, F. Henneberger, and J. Voigt, Phys. Status Solidi B **119**, 291 (1983).

[11] J. Gutowski, Phys. Rev. B **31**, 3611 (1985).

[12] J. Gutowski, Solid State Commun. **58**, 523 (1986).

[13] A. Roussel, thesis for diploma, Technische Universität Berlin, 1979 (unpublished).

[14] I. Broser and J. Gutowski, 2nd International Conference on II–VI Compounds, Aussois, France, 1985 [J. Cryst. Growth **72**, 313 (1985)].

[15] D. G. Thomas and J. J. Hopfield, Phys. Rev. B **128**, 2135 (1962).

[16] P. Loose, thesis for diploma, Technische Universität Berlin, 1975 (unpublished).

[17] M. Rosenzweig, Ph. D. thesis, Technische Universität Berlin, 1982.

[18] B. Stébé, F. Dujardin, and G. Munschy, *Proceedings of the International Conference on the Application of High Magnetic Fields in Semiconductors, Grenoble, France 1982,* Vol. 177 of *Lecture Notes in Physics,* edited by G. Landwehr (Springer, Berlin, 1983), p. 276.

[19] B. Stébé and G. Munschy, Solid State Commun. **35**, 557 (1980), and the literature cited therein.